

# Design of Nanocomposites by Vapor-Phase Assisted Surface Polymerization

Yoshito Andou,<sup>†</sup> Jae-Mun Jeong,<sup>†</sup> Shigehiro Hiki,<sup>†</sup> Haruo Nishida,<sup>\*,‡</sup> and Takeshi Endo<sup>\*,†</sup>

*HENKEL Research Center of Advanced Technology, Molecular Engineering Institute, Kinki University, 11-6 Kayanomori, Iizuka, Fukuoka 820-8555, Japan, and Eco-Town Collaborative R&D Center for the Environment and Recycling, Kyushu Institute of Technology, 2-4 Hibikino, Wakamatsu-ku, Kitakyushu, Fukuoka 808-0196, Japan*

Received July 12, 2008; Revised Manuscript Received December 31, 2008

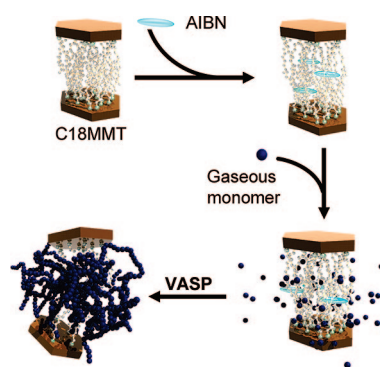
**ABSTRACT:** Exfoliated polymer/clay nanocomposites with high clay contents were facilely constructed by the vapor-phase assisted surface polymerization of methyl methacrylate (MMA) with montmorillonite premodified with a trimethylstearyl ammonium salt and a free radical initiator: 2,2'-azobis(isobutyronitrile). This method required only premodified MMT and vaporized vinyl monomer without any prehomogenizing and postpolymerization processes. The exfoliated structure of the nanocomposites, which was confirmed by X-ray diffraction analysis, was retained even after melt processing.

## Introduction

Vapor-phase assisted surface polymerization (VASP) technique has been developed as the simplest method for constructing micro architectures on solid substrate surfaces with the advantages of being solventless and precise.<sup>1</sup> The VASP technique has other advantages commending it for the construction of fine structured composites<sup>2</sup> and coatings,<sup>3</sup> arising from/at the gaps and spaces within the solid substrate. When these gaps and spaces are wider than the size of monomer molecule, the vaporized monomer can diffuse and penetrate interstitially within the solid substrates. After the diffusion and adsorption on the interstitial surfaces, the monomers polymerize in a manner of “pseudo-grafting from” the substrate surfaces. Polymer chains then grow on the surfaces by filling the spaces, giving a superior anchoring effect, with excellent binding strength at the polymer/substrate interface. Moreover, the growing chain ends, which showed a living nature even when a convenient free radical initiator, azobis(isobutyronitrile) (AIBN), was used as an initiator, enabled block copolymers to form.<sup>1,4</sup> This VASP technique has great potential in the construction of nanocomposites by combinations with inorganic materials having nanoscale structures and can proceed in the simplest manner without any solvent.

The polymer–clay nanocomposites, over the last 15 years, have been widely investigated as materials exhibiting superior properties, such as high modulus, increased thermal stability, and good gas-barrier characteristics.<sup>5</sup> Their development started from the nylon/clay hybrid found by Kamigaito et al.<sup>6</sup> and has since extended to various combinations of monomer/nanofiller using more controllable methods.<sup>7</sup> Their unique properties, with applications to automotive, mechanical, and biomedical devices, have attracted much attention from many researchers and companies.<sup>5,8</sup> The preparation of polymer/clay nanocomposites utilizes bulk, solution, emulsion, and suspension polymerization methods of vinyl and cyclic monomers,<sup>9</sup> together with melt blending.<sup>10</sup> Resulting nanocomposites have two types of structure: intercalated and exfoliated.<sup>5</sup> In spite of the remarkable

**Scheme 1. Exfoliation of Silicate Layers of Clay by VASP**



developments achieved in the preparation techniques of nanocomposites, there are still some problems associated with the liquid processes involved in nanocomposite preparation, such as the requirement of a large amount of aqueous/organic solvent, the aggregation of clay due to insufficient affinity with the monomer, and the lower level of dispersibility in matrix polymers.<sup>11</sup>

PMMA is a transparent, hard, and stiff material with excellent ultraviolet stability, low water absorption, and outstanding outdoor weathering properties. In previous reports, PMMA–clay nanocomposites have been prepared by in situ intercalative polymerization,<sup>12</sup> emulsion polymerization,<sup>13,14</sup> solution polymerization,<sup>14</sup> suspension polymerization,<sup>15,16</sup> and bulk polymerization.<sup>15–18</sup> To achieve the exfoliation, silicate-anchored initiators<sup>7,11</sup> and comonomers having ammonium groups<sup>7,19</sup> have been used to tether the chain ends or internal units to the silicate surfaces. However, there have been few studies of nanocomposite exfoliated by the simplest free radical polymerization without any pretreatment for the homogenization in a liquid phase.

In this paper, the simplest and highly effective synthetic method of vinyl polymer/clay nanocomposites is achieved by using the VASP technique. The nanocomposite production by VASP exhibits a particular exfoliation behavior of the silicate layers compared with previous liquid methods. Since the gaseous monomer can diffuse into any narrow spaces regardless of any affinity between monomer and clay, and, when clay impregnated

\* To whom correspondence should be addressed. Haruo Nishida, Tel/Fax +81-93-695-6233(H.N.); +81-948-22-5706(T.E.). E-mail: nishida@lsse.kyutech.ac.jp (H.N.); tendo@me-henkel.fuk.kindai.ac.jp (T.E.).

<sup>†</sup> Kinki University.

<sup>‡</sup> Kyushu Institute of Technology.

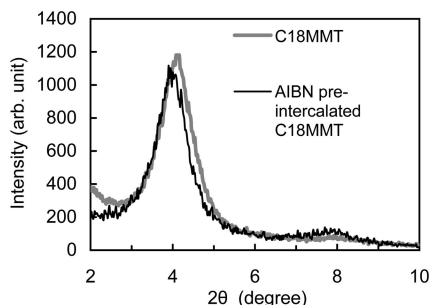


**Figure 1.** XRD patterns of surfactant modified clay before and after AIBN preintercalation.

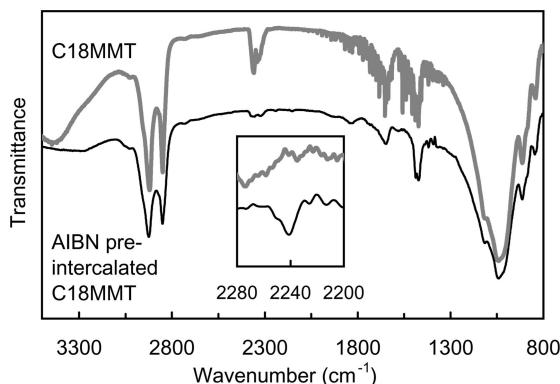


**Figure 2.** FTIR spectra of C18MMT and AIBN preintercalated C18MMT after washing with  $\text{CHCl}_3$ .

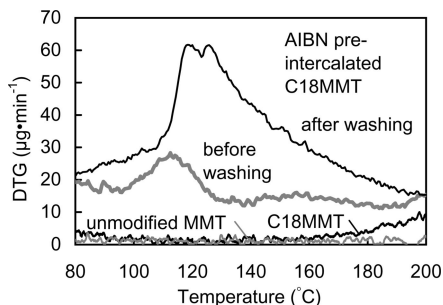


**Figure 3.** DTG thermograms of unmodified MMT, C18MMT, and AIBN preintercalated C18MMT after washing with  $\text{CHCl}_3$ .

by an initiator is used, VASP must proceed by pseudo-“grafting from” the silicate layer surfaces, enlarging the  $d$  spacing of the layers (Scheme 1).

## Experimental Section

**Materials.** Monomer, methyl methacrylate (MMA, 99.0%), from Tokyo Chemical Industry Co., Ltd., was purified by distillation under reduced pressure over  $\text{CaH}_2$  just before polymerization. Initiator, 2,2'-azobis(isobutyronitrile) (AIBN, >99%) was purchased from Otsuka Chemical Inc. and crystallized from methanol. Polymerization inhibitor, 4-*tert*-butylpyrocatechol (>98%) was purchased from Wako Pure Chemical Industries, Ltd. (Wako) and used as received. Substrate, organophilic montmorillonite (C18MMT,  $d$  spacing 2.2 nm (Figure 1)), which was modified with dimethylstearyl-ammonium chloride, was used as received from Kunimine Industries Co., Ltd. Poly(methyl methacrylate) (PMMA,  $M_n$   $0.5 \times 10^5$ ,  $M_w$   $0.7 \times 10^5$ ) was purchased from Wako and used as received. All other reagents, such as acetone (>99%), chloroform ( $\text{CHCl}_3$ , >99.0%, HPLC grade), and methanol (>99%) were commercially obtained and purified by distillation.

## Typical Procedure of Intercalation of Initiator into C18MMT.

Before the vapor-phase assisted surface polymerization (VASP), to intercalate an initiator, 2,2'-azobis(isobutyronitrile) (AIBN), into the silicate layers, C18MMT (1.54 g) was pretreated with a 1 mM acetone solution (500 mL) of AIBN at a 1/30 weight ratio to C18MMT at 25 °C for 0.5 h under stirring. After the pretreatment, acetone was removed under vacuum at room temperature, resulting in the production of C18MMT preintercalated with AIBN. The produced C18MMT was analyzed with XRD to measure the  $d$  spacing of the silicate layers.

Other AIBN-preintercalated C18MMTs with different weight ratios (1/15–1/100 (wt/wt)) of AIBN and C18MMT were also prepared in the same manner (Table S1, Supporting Information).

**Typical Procedure of VASP.** A typical VASP of MMA was carried out in an H-shaped glass tube reactor with a vacuum cock. The C18MMT preintercalated with AIBN (100 mg) was measured into a glass pan (bottom surface area: 154  $\text{mm}^2$ ), and the glass pan was set in the bottom of one of the legs of the H-shaped glass tube reactor. MMA (2.0 mL) and 4-*tert*-butylpyrocatechol (20 mg,  $1.2 \times 10^{-4}$  mol) were introduced into the bottom of the other leg. The reactor was degassed by three freeze–pump–thaw cycles and then sealed under a saturated atmosphere of vaporized MMA. Polymerization was carried out at 70 °C for 3 h under a saturated vapor pressure of  $3.27 \times 10^4$  Pa in a thermostatted oven.

After the reaction, the sample, which was expanded by newly intercalated polymer chains, was dried to remove the adsorbed MMA in vacuo and weighed to obtain 830 mg of PMMA/C18MMT composite. The produced composite was analyzed intact with XRD to measure the  $d$  spacing of the silicate layers.

Free polymers in PMMA/C18MMT composites were extracted using tetrahydrofuran (THF) as a good solvent overnight at room temperature. The THF solution was repeatedly filtered to ensure the removal of the clay, and then extracted polymer was precipitated with methanol. The isolated polymers were dried and analyzed by Fourier transform infrared (FTIR),  $^1\text{H}$  NMR, and size-exclusion chromatography (SEC).

**Melt Processing.** Melt processing of PMMA/C18MMT composites was carried out by compression molding, in which composites were preheated for 2 min in a compressor heated at 210 °C and followed by heat-pressing for 3 min at the same temperature to obtain a thin film (thickness ca. 100  $\mu\text{m}$ ).

**Characterization Methods.** X-ray diffraction (XRD) patterns were obtained by using a Rigaku diffractometer equipped with a  $\text{Cu K}\alpha$  generator ( $\lambda = 0.1541$  nm) under the following conditions: slit width, 0.30 mm; generator current, 16 mA; voltage, 30 kV; and scanning rate, 2  $\text{degree} \cdot \text{min}^{-1}$ .

$^1\text{H}$  NMR spectra were recorded on a 300 MHz JEOL AL-300 MHz spectrometer. Chloroform- $d$  ( $\text{CDCl}_3$ ) was used as a solvent. Chemical shifts were reported as  $\delta$  values (ppm) relative to internal tetramethylsilane (TMS) in  $\text{CDCl}_3$  unless otherwise noted. FTIR spectroscopy was performed using a JASCO FTIR 460 plus spectrometer. Transmission spectra were recorded from KBr plates, on which surfaces polymer samples were coated from chloroform solutions.

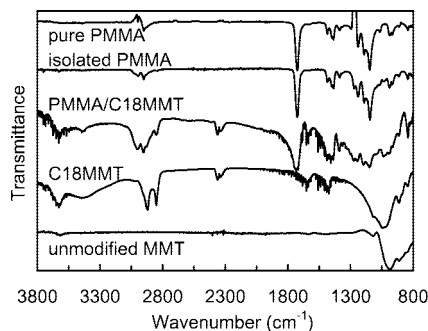
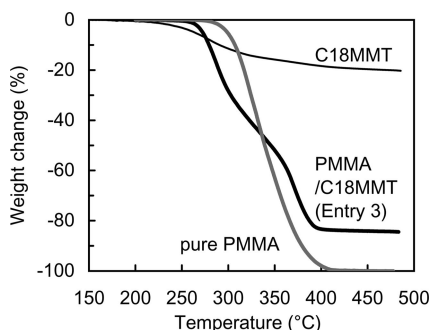
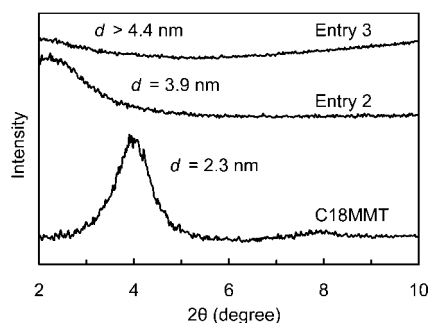
Molecular weights of polymers were measured on a TOSOH HLC-8220 SEC system with refractive index (RI) and ultraviolet (UV,  $\lambda = 254$  nm) detectors under the following conditions: TSKgel Super HM-H linear column (linearity range,  $1 \times 10^3$ – $8 \times 10^6$ ; molecular weight exclusion limit,  $4 \times 10^8$ ), THF eluent at a flow rate of 0.6  $\text{mL} \cdot \text{min}^{-1}$ , and column temperature of 40 °C. The calibration curves for SEC analysis were obtained using polystyrene standards with a low polydispersity ( $5.0 \times 10^2$ ,  $1.05 \times 10^3$ ,  $2.5 \times 10^3$ ,  $5.87 \times 10^3$ ,  $9.49 \times 10^3$ ,  $1.71 \times 10^4$ ,  $3.72 \times 10^4$ ,  $9.89 \times 10^4$ ,  $1.89 \times 10^5$ ,  $3.97 \times 10^5$ ,  $7.07 \times 10^5$ ,  $1.11 \times 10^6$ , TOSOH Corporation).

Thermogravimetric/differential thermal analysis (TG/DTA) was performed on a TG/DTA 6200 (Seiko Instruments Inc.) under a nitrogen flow with a heating rate of 10  $^\circ\text{C} \cdot \text{min}^{-1}$ .

**Table 1. VASP of MMA on Original C18MMT and AIBN Preintercalated C18MMT<sup>a</sup>**

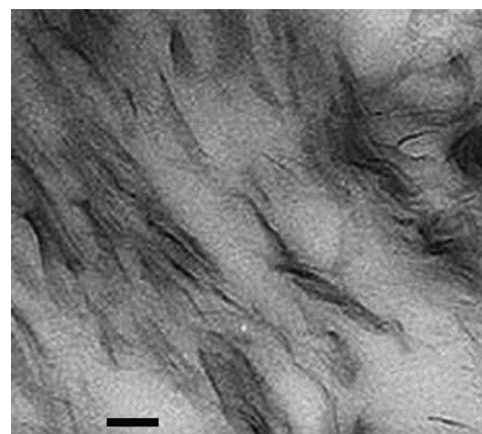
entry	organophilic clay <sup>b</sup>	time (h)	product (mg)	polymer yield (mg)	ratio of free polymer <sup>c</sup> (%)	$M_n^d$	poly dispersity	<i>d</i> -spacing (nm)
1	C18MMT	3	100	0				2.3
2	C18MMT/AIBN	1.5	380	280	n.m. <sup>e</sup>	$1.5 \times 10^6$	1.5	3.9
3	C18MMT/AIBN	3	830	730	77.2	$0.7 \times 10^6$	2.7	>4.4 <sup>f</sup>

<sup>a</sup> Polymerization conditions: monomer, MMA (2.0 mL); substrate, C18MMT (100 mg); at 70 °C. <sup>b</sup> Composition: C18MMT:AIBN = 30:1 (wt/wt). <sup>c</sup> Free polymer was extracted using tetrahydrofuran overnight at room temperature. <sup>d</sup> Number average molecular weight determined by SEC relative to polystyrene standards. <sup>e</sup> not measured. <sup>f</sup> No diffraction peak in a range of  $2\theta = 2\text{--}10^\circ$ , which is indicative of exfoliated structure.

**Figure 4.** FTIR spectra of unmodified MMT, C18MMT, PMMA/C18MMT (entry 3 in Table 1), isolated PMMA, and pure PMMA.**Figure 5.** TG profiles of C18MMT, PMMA/C18MMT (entry 3 in Table 1), and pure PMMA. Heating rate: 10 °C·min<sup>-1</sup> under a N<sub>2</sub> flow (100 mL·min<sup>-1</sup>).**Figure 6.** Comparison of XRD patterns of C18MMT and products after VASP of MMA.

## Results and Discussion

**Pretreatment of MMT with AIBN.** Montmorillonite (MMT, *d* spacing calculated from (001) basal plane diffraction: 1.2 nm) is one typical kind of clay. An organophilic MMT modified with dimethylstearyl-ammonium chloride (C18MMT, *d* spacing: 2.2 nm) was pretreated with a 1 mM acetone solution of an initiator AIBN at a 1/30 weight ratio to C18MMT to intercalate AIBN into the silicate layers.<sup>10</sup> After removing acetone, the pretreated C18MMT was analyzed by XRD, resulting in an average enlarging of the *d* spacing by  $0.09 \pm 0.03$  (SD) nm (Figure 1). To confirm the intercalation of AIBN molecules in interlayer spaces, the initiators attached on outside surfaces of the AIBN-pretreated C18MMT was washed out with CHCl<sub>3</sub>

**Figure 7.** TEM image of melt-processed PMMA/C18MMT nanocomposite thin film. Bar: 50 nm.

under vigorous stirring, in which the C18MMT was not swollen. The C18MMT samples before and after the AIBN treatment and CHCl<sub>3</sub> washing were analyzed by FTIR and TG/DTA (Figures 2 and 3). FTIR spectrum and DTG thermogram of the washed C18MMT showed a characteristic peak at 2242 cm<sup>-1</sup> assigned to  $\nu_{N=N}$  of AIBN and an exothermic peak in 110–150 °C attributed to the thermal degradation of AIBN, whereas no characteristic peak and signal in FTIR spectrum and DTG thermogram, respectively, for unmodified MMT and C18MMT before AIBN-treatment was observed. DTG signals attributable to free AIBN adsorbed on outside surfaces of C18MMT and dimethylstearyl ammonium chloride attached on MMT platelet surfaces were observed at temperatures in a range of 100–130 °C and higher than 200 °C, respectively. These results indicate that AIBN molecules were intercalated between the C18MMT silicate layers.<sup>11</sup> Therefore, radical species generated from the intercalated AIBN could diffuse into/out of the silicate layers of the silicate layers.

**VASP of MMA with C18MMTs.** VASP of MMA was conducted with original C18MMT and the AIBN-preintercalated C18MMT at 70 °C under a saturated vapor pressure of MMA (32.7 kPa) without any prehomogenizing process. Because the long carbon chains of the organic surfactant on C18MMT platelet surfaces provide a larger and more organophilic interlayer space than that of the original MMT, organic monomers, especially gaseous monomers, can easily diffuse into the interlayer spaces and undergo polymerization.<sup>20</sup> During the VASP, no change was observed on the original C18MMT (entry 1 in Table 1), but the AIBN-intercalated C18MMT powder gradually enlarged with the growth of polymer chains and finally gave expanded powdery products (entries 2 and 3). From the increase in weight of the substrate, it was found that the product after the reaction for 3 h comprised 89.1 wt % of newly generated material and 10.9 wt % of the original C18MMT.

**Characterization of Composites.** Analytical results of the as-polymerized products by FTIR, TG, and XRD are shown in Figures 4, 5, and 6, respectively. FTIR spectrum in Figure 4 showed a characteristic peak of PMMA at 1747 cm<sup>-1</sup> assigned to  $\nu_{C=O}$ ; this peak being broadened as compared to the same



peak of pure PMMA, indicating a hydrogen bond interaction between the carbonyl group of the polymer and the clay surface.<sup>21</sup> TG profile of the as-polymerized product PMMA/C18MMT in Figure 5 exhibited two-step weight loss behavior due to the degradation of PMMA ingredient, showing a similar composition ratio to that calculated from the increase in weight during VASP, whereas a pure PMMA showed a smooth one-step degradation profile. This TG result of PMMA/C18MMT suggests that the polymeric product consists of two kinds of PMMA existing in different circumstances and/or having different molecular weights. VASP of MMA must occur in two circumstances such as inside and outside of silicate layers. Each polymerization may proceed by different kinetics having, for example, different chain growth rates and/or termination/transfer rates, resulting in the production of a polymer having a high polydispersity value (entry 3 in Table 1).

XRD patterns of the products were shown in Figure 6. Although the pattern of the product after VASP for 1.5 h showed a peak at  $2\theta = 2.27^\circ$  (entry 2 in Table 1), no diffraction peak but instead a broad slope directed to a lower  $2\theta$  area than  $2^\circ$  was observed in the pattern of the product after VASP for 3 h in a  $2\theta$  range of  $2\sim 10^\circ$ . This means that after the reaction had continued for 3 h the averaged  $d$  spacing between the silicate layers of MMT had become larger than 4.4 nm and the silicate layers were mostly exfoliated. This result shows the very simple and convenient production of PMMA/MMT nanocomposite.<sup>19</sup>

To confirm that the newly generated material on C18MMT was indeed PMMA, the material in the product of entry 3 in Table 1 was extracted using tetrahydrofuran and the isolated material was analyzed by FTIR,  $^1\text{H}$  NMR, and SEC. Results are shown in Figures 4 and S1 in Supporting Information, and Table 1. FTIR and  $^1\text{H}$  NMR spectra of the isolated material showed the same spectra as that of pure PMMA, for example, characteristic peaks of PMMA at  $1726\text{ cm}^{-1}$  and 3.65 ppm as a singlet signal assigned to  $\nu_{\text{C=O}}$  and  $-\text{COOCH}_3$ , respectively. From SEC analysis, number and weight average molecular weights of the isolated PMMA were  $0.7 \times 10^6$  and  $1.9 \times 10^6$ , respectively.

The extracted free polymer was 77.2 wt % of total accumulation (entry 3 in Table 1). Therefore, it is considered that at least 22.8 wt % of the accumulation was made up of PMMA chains grown in interlayer spaces and that these chains might have grafted on the substrate surfaces.

**Structure of Nanocomposites.** To determine the dispersion of individual silicate platelets in the PMMA matrix, TEM images of the PMMA/MMT nanocomposite were observed after melt processing the as-polymerized product (entry 3 in Table 1) into a thin film. A typical TEM image of the thin film is shown in Figure 7. Even after the melt processing, the morphology of silicate layers that had mostly been exfoliated was preserved. This means that the polymer chains remained attached on the silicate surfaces to retain the dispersion of individual silicate platelets in the polymer matrix. Thus, the VASP technique is a workable method for destroying the layered structure of MMT, achieving a homogeneous dispersion of the silicate platelets in the PMMA matrix and retaining the dispersion even after the melt processing of the composite.

The VASP technique is probably not only the simplest, but also one of the most effective methods for achieving the exfoliation of MMT. The VASP requires the minimum amount of monomer and time, because all the unreacted monomers are easily recovered and some time-consuming processes before and after the polymerization such as ultrasonication, desolvation, crushing the product, etc. are avoidable. The growing polymer chains during the VASP effectively delaminated the silicate layers after a reaction time of only 3 h, a shorter time than that generally required for liquid processes (4–72 h), and even under

low concentrations of AIBN (Table S1, entries 6 and 7 in Supporting Information). Actually, when a solution polymerization was carried out in toluene with the same AIBN-intercalated C18MMT at  $85^\circ\text{C}$  for 3 h as a comparison, obtained product was an intercalated nanocomposite ( $d$  spacing 3.3 nm) and not exfoliated (Table S2 and Figure S2 in Supporting Information). This means that the solution polymerization requires more severe conditions to give exfoliated layered structure.

These attractive characteristics of the simplicity and effectiveness of VASP add value to its other features of being solventless, having no prehomogenous process, and involving a free combination of monomer and substrate.

## Conclusion

A highly effective and the simplest construction method of vinyl polymer–clay nanocomposite was developed by using VASP technique. This approach provides us with a novel concept in nanocomposite construction: solventless, minimum use of resources, effective development of the function, and so on. If the processes of preorganization and initiator-charging on the silicate layer surfaces are achieved in a gaseous phase, this total VASP process can be expected to extend to applications in many fields. Efforts directed toward this goal are currently underway.

**Acknowledgment.** This work was performed under the sponsorship of Henkel KGA in German. We thank PS Japan Corporation for providing the transmission electron micrograph.

**Supporting Information Available:**  $^1\text{H}$  NMR spectrum of isolated free PMMA, VASP results using other AIBN-preintercalated C18MMTs with different weight ratios (AIBN/C18MMT = 1/15–1/100 (wt/wt)), and comparative results of solution polymerization. This material is available free of charge via the Internet at <http://pubs.acs.org>.

## References and Notes

- (1) (a) Fu, D.; Weng, L.-T.; Du, B.; Tsui, O. K. C.; Xu, B. *Adv. Mater.* **2002**, *14*, 339. (b) Wang, Y.; Chang, Y. C. *Adv. Mater.* **2003**, *15*, 290. (c) Gu, H.; Xu, C.; Weng, L.-T.; Xu, B. *J. Am. Chem. Soc.* **2003**, *125*, 9256. (d) Yasutake, M.; Hiki, S.; Andou, Y.; Nishida, H.; Endo, T. *Macromolecules* **2003**, *36*, 5974. (e) Chan, K.; Gleason, K. K. *Langmuir* **2005**, *21*, 8930. (f) Lau, K. K. S.; Gleason, K. K. *Adv. Mater.* **2006**, *18*, 1972. (g) Andou, Y.; Nishida, H.; Endo, T. *Chem. Commun.* **2006**, 5018. (h) Andou, Y.; Yasutake, M.; Nishida, H.; Endo, T. *J. Photopolym. Sci. Technol.* **2007**, *20*, 523.
- (2) Nishida, H.; Yamashita, M.; Andou, Y.; Jeong, J.-M.; Endo, T. *Macromol. Mater. Eng.* **2005**, *290*, 848.
- (3) (a) Lau, K. K. S.; Bico, J.; Teo, K. B. K.; Chhowalla, M.; Amaratunga, G. A. J.; Milne, W. I.; McKinley, G. H.; Gleason, K. K. *Nano Lett.* **2003**, *3*, 1701. (b) Gupta, M.; Kapur, V.; Pinkerton, N. M.; Gleason, K. K. *Chem. Mater.* **2008**, *20*, 1646.
- (4) (a) Yasutake, M.; Andou, Y.; Hiki, S.; Nishida, H.; Endo, T. *Macromol. Chem. Phys.* **2004**, *205*, 492. (b) Yasutake, M.; Andou, Y.; Hiki, S.; Nishida, H.; Endo, T. *J. Polym. Sci., Part A: Polym. Chem.* **2004**, *42*, 2621.
- (5) (a) Alexandre, M.; Dubois, P. *Mater. Sci. Eng.* **2000**, *R28*, 1. (b) Giannelis, E. P.; Krishnamoorti, R.; Manias, E. *Adv. Polym. Sci.* **1999**, *138*, 107. (c) Kawasumi, M. *J. Polym. Sci., Part A: Polym. Chem.* **2004**, *42*, 819.
- (6) (a) Kojima, Y.; Usuki, A.; Kawasumi, M.; Okada, A.; Kurauchi, T.; Kamigaito, O. *J. Polym. Sci., Part A: Polym. Chem.* **1993**, *31*, 983. (b) Usuki, A.; Kawasumi, M.; Kojima, Y.; Okada, A.; Kurauchi, T.; Kamigaito, O. *J. Mater. Res.* **1993**, *8*, 1174.
- (7) (a) Messersmith, P.; Giannelis, E. *J. Polym. Sci., Part A: Polym. Chem.* **1995**, *33*, 1047. (b) Weimer, M. W.; Chen, H.; Giannelis, E. P.; Sogah, D. Y. *J. Am. Chem. Soc.* **1999**, *121*, 1615. (c) Ma, J.; Qi, Z.; Hu, Y. *J. Appl. Polym. Sci.* **2001**, *82*, 3611. (d) Manias, E.; Touny, A.; Wu, L.; Strawhecker, K.; Lu, B.; Chung, T. *Chem. Mater.* **2001**, *13*, 3516. (e) Di, J.; Sogah, D. Y. *Macromolecules* **2006**, *39*, 5052. (f) Shi, Y.; Peterson, S.; Sogah, D. Y. *Chem. Mater.* **2007**, *19*, 1552.
- (8) Haraguchi, K.; Takehisa, T. *Adv. Mater.* **2002**, *14*, 1120.

- (9) (a) Lee, D.; Jang, L. *J. Appl. Polym. Sci.* **1996**, *61*, 1117. (b) Huang, X.; Brittain, W. *Macromolecules* **2001**, *34*, 3255. (c) Bandyopadhyay, S.; Giannelis, E. P.; Hsieh, A. *Polym. Mater. Sci. Eng.* **2000**, *82*, 208.
- (10) Okamoto, M.; Morita, S.; Taguchi, H.; Kim, Y.; Kotaka, T.; Tateyama, H. *Polymer* **2000**, *41*, 3887.
- (11) (a) Huang, X.; Brittain, W. J. *Macromolecules* **2001**, *34*, 3253. (b) Fan, X.; Xia, C.; Advincula, R. C. *Langmuir* **2003**, *19*, 4381. (c) Fan, X.; Xia, C.; Advincula, R. C. *Langmuir* **2005**, *21*, 2537. (d) Di, J.; Sogah, D. Y. *Macromolecules* **2006**, *39*, 1020.
- (12) Krishnamoorti, R.; Vaia, R. A.; Giannelis, E. P. *Chem. Mater.* **1996**, *8*, 1728.
- (13) Li, Y.; Zhao, B.; Xie, S.; Zhang, S. *Polym. Int.* **2003**, *52*, 892.
- (14) Xie, T.; Yang, G.; Fang, X.; Ou, Y. *J. Appl. Polym. Sci.* **2003**, *89*, 2256.
- (15) Huang, X.; Brittain, W. J. *Macromolecules* **2001**, *34*, 3255.
- (16) Wang, D.; Zhu, J.; Yao, Q.; Wilkie, C. A. *Chem. Mater.* **2002**, *14*, 3837.
- (17) Qu, X.; Guan, T. G.; Liu, G.; She, Q.; Zhang, L. *J. Appl. Polym. Sci.* **2005**, *97*, 348.
- (18) Lee, D. C.; Jang, L. W. *J. Appl. Polym. Sci.* **1996**, *61*, 1117.
- (19) (a) Fu, X.; Qutubuddin, S. *Polymer* **2001**, *42*, 807. (b) Zeng, C.; Lee, L. J. *Macromolecules* **2001**, *34*, 4098. (c) Wang, D.; Zhu, J.; Yao, Q.; Wilkie, C. A. *Chem. Mater.* **2002**, *14*, 3837.
- (20) Choi, Y.; Ham, H.; Chung, I. *Chem. Mater.* **2004**, *16*, 2522.
- (21) Zhao, Q.; Samulski, E. T. *Macromolecules* **2005**, *38*, 7967.

MA802453N